Available online at www.sciencedirect.com
SCIENCE DIRECT
Materials Research Bulletin 41 (2006) 899–904
Materials Research Bulletin
www.elsevier.com/locate/matresbu

Novel rosette-shaped CdS microparticle with high surface area fabricated by lyotropic liquid crystal templating

Sung-Jae Im, Weon-Sik Chae, Sang-Wook Lee, Yong-Rok Kim *

Department of Chemistry and Photon Applied Functional Molecule Research Laboratory, Yonsei University, Seoul 120-749, South Korea

Received 16 September 2005; accepted 30 September 2005
Available online 19 October 2005

Abstract

Semiconductor CdS microparticle covered with wrinkle-like nanotexture was prepared under ambient condition by using the lyotropic liquid crystal mesophase as a structural template. The prepared CdS microparticle resembles a rosette shape with a diameter of 0.5–1.5 μm and the wrinkle-like nanotexture on its surface. This rosette-shaped CdS consists of small nanocrystals with a diameter of ~4 nm, and the nanocrystal building block has the zinc-blende crystal structure. The characteristic band-to-band absorption and near band-edge emission are observed in this unique semiconductor particle. Nitrogen gas physisorption measurement reveals that the material has the high BET surface area of 38 $m^2 g^{-1}$ and nanoporous nature.

Keywords: A. Semiconductors; A. Chalcogenides; A. Nanostructures; B. Chemical synthesis; D. Optical properties

1. Introduction

Large interests in nanomaterials have recently been given due to their promising potentials for various applications such as smart optics, integrated electronics, storage medium, solar cell, and catalyst [1–5]. Among various synthetic strategies for nanomaterials, the lyotropic liquid crystal (LLC) templating method is a convenient way for the preparation of the specific nanostructures since the unique ability of the LLC provides the well-defined nanostructures of vesicular micelle, cubic, hexagonal, and lamellar mesophases depending on the surfactant types and the concentrations.

Recently, various nanostructures have been fabricated by using the LLC templating method: Semiconductor nanowire was synthesized from an inverted hexagonal LLC template induced by an oligo(ethylene oxide)oleylether amphiphile [6], and the novel nanostructures of the flake- and disk-shapes were prepared by using the microemulsions consisting of cationic surfactants under hydrothermal conditions [7]. Furthermore, the mesophased semiconductor superstructures were fabricated by direct templating of the LLC phases of the hexagonal, lamellar, and cubic structures, where the products showed the similar structural features with the utilized mesophase templates [8].

In this study, we report the synthesis of rosette-shaped CdS microparticles by using the Brij-56 solution system as a structure directing LLC template. The resulting spherical product has the wrinkle-like nanotexture on its surface. This

* Corresponding author. Tel.: +82 2 2123 2646; fax: +82 2 364 7050.
E-mail address: yrkim@yonsei.ac.kr (Y.-R. Kim).

0025-5408/$ – see front matter
doi:10.1016/j.materresbull.2005.09.023

unique CdS microparticle shows a high specific surface area, nanoporous nature, and characteristic optical response in visible spectral region.

2. Experimental

In a typical procedure, 3.20 g of Brij-56 ($C_{16}H_{33}(OCH_2CH_2)_n(OH)$, $n = \sim 10$, Aldrich) was dissolved in 0.80 g of ethanol (Merck KGaA, Germany). Subsequently, 0.94 g of cadmium nitrate tetrahydrate (Kanto Chemical, Japan) was added to the above ethanol solution with stirring at room temperature for 1 h. The final solution was transferred into a 20 ml borosilicate glass vial and sealed tightly with a commercial paraffin film. The sealed vial was then placed in H_2S environment and the entire gel was gradually turned to yellow within 3 days. The resulting precipitate was removed from the vial and repeatedly washed and centrifuged with the mixed solution of diethyl ether and ethanol (50:50 volume ratio) to remove the residual Brij-56 and other ionic species. After the product was dried at 60 °C for 24 h, they were dipped in an acidic ethanol solution (10 ml of 2 M acetic acid mixed with 80 ml of ethanol) and refluxed for 12 h to extract the surfactant molecules from the rosette-shaped CdS particle. Infrared absorption spectra (data not shown) showed that the characteristic –CH_2– stretching bands (2850 and 2920 cm^{-1}) corresponding to the Brij-56 surfactant were drastically reduced in its intensity after the solvent extraction, indicating the effective removal of the surfactant molecules from the CdS precipitate.

For morphological study of the CdS precipitate, field-emission scanning electron microscope (FE-SEM) images were obtained on a microscope (JEOL, JEM-6700F) operated at 15 kV. Transmission electron microscope (TEM) image and energy dispersive X-ray (EDX) spectrum were obtained on a microscope (JEOL, 3011) that was operated at 200 kV with the sample deposited on a carbon coated copper grid. The X-ray diffraction (XRD) patterns for the powder samples were recorded on a diffractometer (Mac Science, M03XHF[22]) with Cu Kα (λ = 1.5406 Å) radiation. The nitrogen gas adsorption measurement was conducted on an adsorption analyzer (Micromeritics, ASAP-2010). Infrared absorption spectra were obtained on a spectrometer (Nicolet, Avatar-360-FT-IR). UV–vis absorption and photoluminescence (PL) spectra were obtained with an absorption spectrophotometer (Jasco, V-550) and an emission spectrophotometer (Hitachi, F-4500), respectively.

3. Results and discussion

The template structure of the utilized LLC phase was investigated by the X-ray diffraction analysis. The LLC phase which consists of the Brij-56 surfactant, ethanol, and cadmium precursor has two distinct diffractional peaks at 1.45 ° and 4.35 ° in 2θ (Fig. 1a). Since these peaks can reasonably be indexed as (0 0 1) and (0 0 3) miller planes,

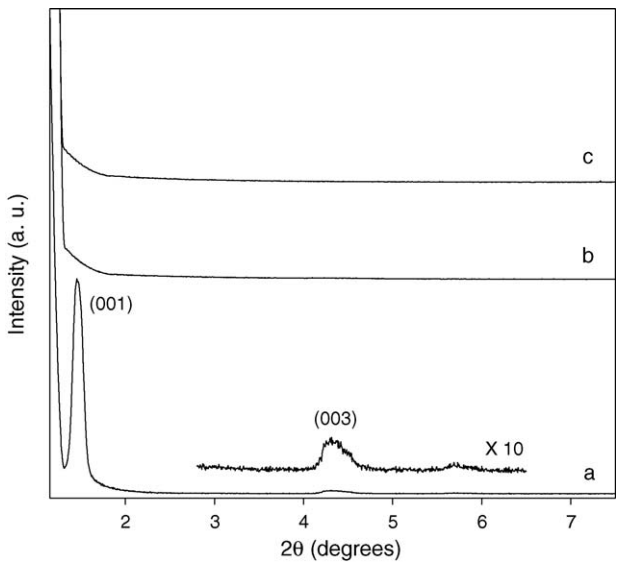

Fig. 1. Small-angle XRD patterns for (a) the lamellar mesophase including cadmium ions, (b) the as-made CdS, and (c) the surfactant-free CdS.

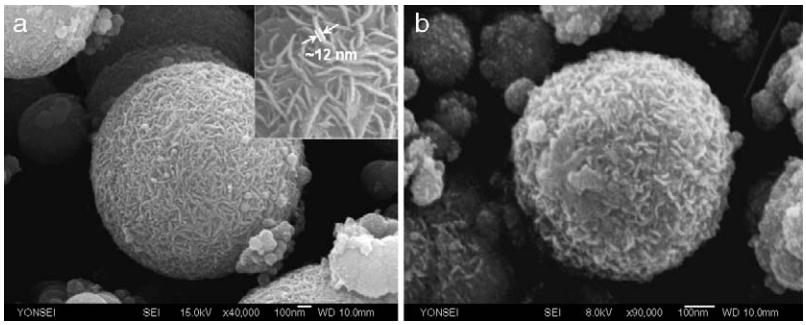

Fig. 2. SEM images for (a) the as-made CdS and (b) the surfactant-free CdS. Inset is the magnified surface image for the as-made one.

respectively, the structure of the utilized LLC system containing cadmium precursor is assigned to a lamellar mesophase with the $d_{(0\ 0\ 1)}$-spacing of 6.1 nm. In particular, it is noticeable that the (0 0 2) and (0 0 4) planes are not clearly observed in this system. For the ideal two-phase lamellar system, the Bragg peaks occur at a series of the q-values satisfying $q = 2\pi n/d$, and the intensity of the nth order peak is proportional to $\sin^2(\pi n\phi_A)/n^2$, where $\phi_A(=d_A/d)$ is the volume fraction of one phase [9]. Therefore, one can expect that, when the volumes of the two phases are equal, all even order peaks are reduced to zero intensity. Such absence of the even order peaks in this study implies that the Brij-56 LLC phase possibly has the similar phase volumes for both the nonpolar hydrocarbon phase and the polar phase which includes the ethanol and the cadmium ions.

After slow addition of H_2S gas into the lamellar LLC mesophase including cadmium ions, both the as-made and the template removed CdS do not show any prominent diffractional peak in the similar diffraction range compared with that of the LLC mesophased template. Such disappearance of the LLC diffraction peaks after the formation of CdS within the lamellar LLC mesophase may be caused by the simple formation of the neat spherical particles without the lamellar structure and/or the irregular lamellar structure which can be induced by the structural deformation.

SEM images for the CdS products with and without the surfactant are presented in Fig. 2. The as-made CdS product shows a spherical morphology with the typical size of 0.5–1.5 μm in diameter, and the surface of the CdS products is interestingly covered with wrinkle-like nanotexture. This unique morphology is still maintained after removal of the utilized organic template (Fig. 2b).

As shown in the magnified image of the as-made CdS (inset of Fig. 2a), the wrinkle-like nanotexture with the lateral dimension of ~12 nm is randomly formed at the surface of the CdS microparticle. Such wrinkle-like nanotexture was not observed in the same reaction without the Brij-56 LLC template (data not shown). Therefore, it is considered that this unique wrinkle-like nanotexture is induced by the LLC templating. On the other hand, the core part of the CdS microparticle is shown to be densely agglomerated (Fig. 3). Such results suggest that the templating concept does work only at the outer part of the CdS microparticle during the reaction and, in the core part, the CdS becomes densely aggregated regardless of the templating force.

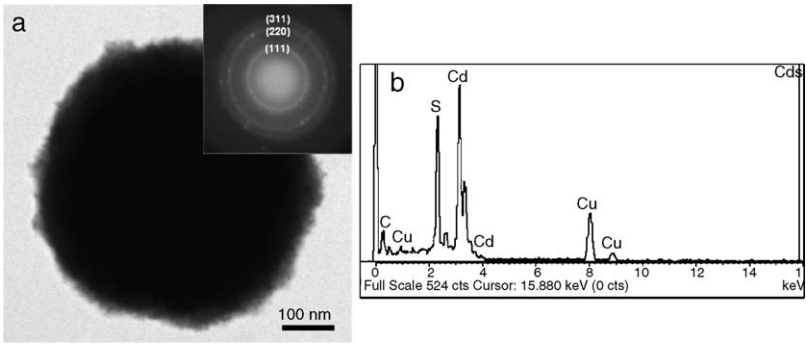

Fig. 3. (a) TEM image for the surfactant-free CdS. Inset shows the electron diffraction pattern. (b) EDX spectrum for the surfactant-free CdS which presents the existence of cadmium and sulfur atoms with the elemental ratio of 1.0:0.9 for Cd:S. The additionally detected elements of carbon and copper from the EDX spectrum are due to the utilized carbon coated copper grid.

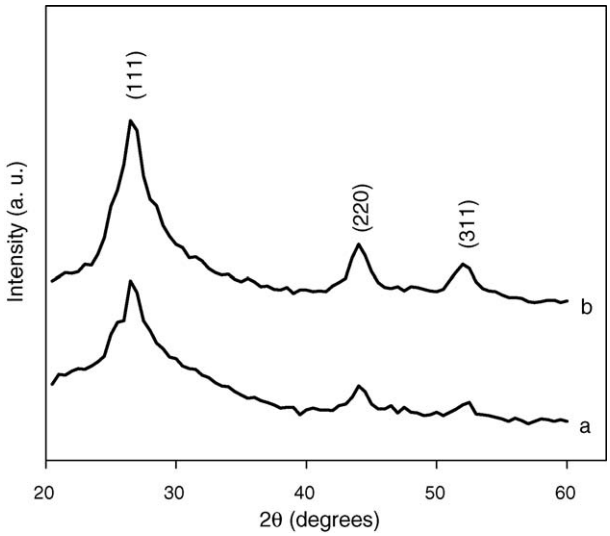

Fig. 4. Wide-angle XRD patterns for (a) the as-made CdS and (b) the surfactant-free CdS.

Previously, it was suggested that the slow release of H_2S was a prerequisite for the formation of the CdS mesophase replicating the supramolecular template without disturbing the mesophase structure [10]. However, although the slow addition of the H_2S was ensured by using a protecting paraffin film which seals the entrance of reaction vial in order to avoid the collapse of the lamellar mesophase template, such disruption in the core part still occurred in this experiment. It indicates that the initial reaction step is somewhat violent enough to overwhelm the formation force of the supramolecular mesophased template, which plausibly results in the dense agglomerate in the core part. Therefore, the wrinkle-like nanotexture appeared at the outer part implies that the templating process may work at the final step of the reaction.

Fig. 4 presents the wide-angle diffractions for the rosette-shaped CdS microparticles. The CdS microparticles show the well-correlated structural feature with the zinc-blende crystal structure (JCPDS card No. 21-829). It is notable that the diffraction peaks are somewhat broad. In general, X-ray diffraction peak becomes to be broadened as the crystal size reduces [11]. Therefore, nanocrystal size can be estimated from the XRD peak broadening by applying the Debye–Scherrer formula, $D = 0.9\lambda/B_w \cos\theta$, where λ is the wavelength (1.54056 Å) of the utilized X-ray source and B_w is the full width at half maximum of a diffraction peak [11–13]. In this study, as the (1 1 1) diffraction peak is applied to the size estimation, the crystal diameters of ~4.0 nm are obtained for both the as-made and the surfactant-free CdS. It indicates that the rosette-shaped CdS with the wrinkle-like nanotexture is a polycrystalline microparticle consisted of a number of small-sized nanocrystals. Such structural property is also well correlated with the observed ring pattern from the electron diffraction analysis which is a typical diffraction pattern for polycrystalline structure (inset of Fig. 3).

Fig. 5 shows the absorption and emission spectra of the surfactant-free CdS microparticle. The absorption spectrum presents the band-gap transition at ~485 nm (2.56 eV). Such blue-shifted absorption compared with the bulk band-gap energy of CdS (2.4 eV) is typically responsible for quantum size effect. Therefore, in this study, the modified effective mass approximation (MEMA) which was proposed by Nosaka was applied to the size estimation [14]. According to the theory, the lowest exciton transition energy (E_{ex}) of a semiconductor nanocrystal with a radius of R is defined as follows:

$$E_{ex} = E_g + V_e + V_h + E_c$$

where E_g is the bulk band-gap energy (2.4 eV), V the kinetic energy for electron and hole in a finite-depth ($V_0 = 3.6$ eV) spherical well which is expressed as $V/V_0 = a + b/\{(V_0 m^*/m_e)^{1/2} R + c\}^2$, and E_c is the Coulomb interaction term ($E_c = -1.786e^2/\varepsilon R$) between the electron and the hole. In this size estimation, the utilized numerical values are of $0.19m_e$, $0.80m_e$, and 5.6 for the m_e^*, m_h^*, and ε, respectively [14]. The resulted diameter of the nanocrystal building-block of the rosette-shaped CdS is estimated to be ~4.5 nm. This estimated size of the nanocrystal from the MEMA shows the consistency with the crystal size (~4 nm) calculated from the XRD analysis.

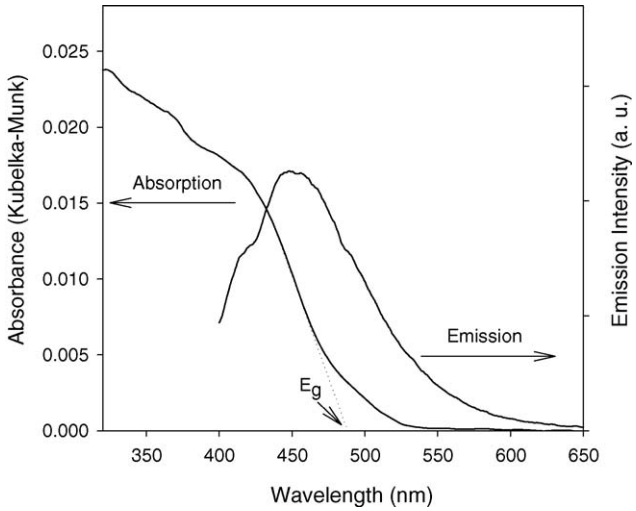

Fig. 5. Absorption and emission spectra for the surfactant-free CdS. The absorption spectrum is obtained by applying the Kubelka–Munk function to the measured diffuse reflectance spectra. The excitation wavelength is 400 nm for the emission spectrum.

In addition to the band-gap transition of the CdS nanocrystal, the extended absorption which approaches to the bulk transition of CdS (520 nm [15]) is also observed. Such observed absorption pattern of the band-gap transition and the extended absorption to the bulk transition may be expected from the nanosize effects [16,17] of the various structural components of the CdS microparticle; the nanocrystal building-blocks which are patterned to the wrinkle-like nanotexture at the surface and the bulky agglomerate in the core. The observed emission spectrum is located near the absorption edge, which originates from the direct exciton recombination and/or shallowly trapped exciton recombination [18,19].

The nitrogen adsorption–desorption isotherm is presented for the surfactant extracted one in Fig. 6. From the result, the Brunauer–Emmett–Teller (BET) surface area is estimated to be 38 $m^2\ g^{-1}$, which is much larger than the expected value (1.25 $m^2\ g^{-1}$) assuming the neat spherical CdS microparticles with 1 μm diameter (the density of 4.82 g/cm^3

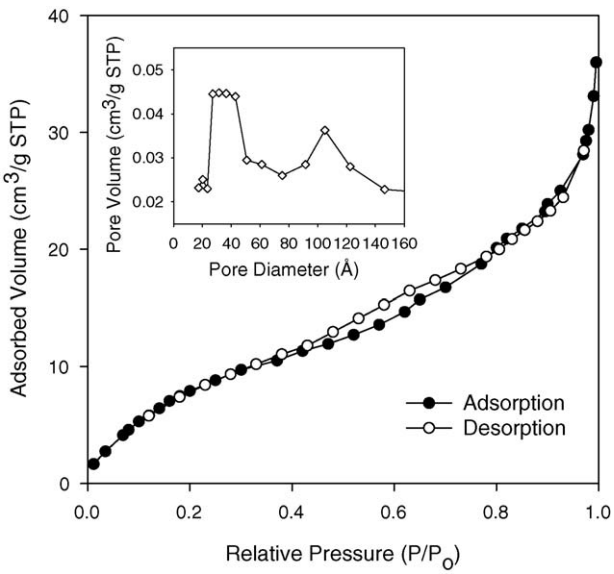

Fig. 6. Nitrogen adsorption–desorption isotherm for the surfactant-free CdS. Inset shows its pore-size distribution derived from the desorption branch.

[20] is used for the estimation). It is also noteworthy that the weak hysteresis is observed around the relative pressure of 0.6, which suggests the existence of nanopores and/or nanocavities inside of the unique CdS microparticle, as similarly with the reports for the disordered or layered nanostructures [21–23]. The major pore diameter estimated by the Barrett–Joyner–Halenda (BJH) method is 3–4 nm from the desorption branch, and the minor pore with a diameter of ~10 nm is also observed (inset of Fig. 6). These bimodal nanopores and/or nanocavities are believed to exist in this wrinkle-like nanotexture which have the irregularly stacked pattern [22,23] at the outer part including the surface. These unique structural characteristics of the rosette-shaped CdS microparticle are possibly responsible for the 30 times higher surface area than that of the neat spherical CdS.

4. Conclusions

Rosette-shaped CdS microparticle was prepared by using an amphiphilic surfactant of Brij-56 as a structure directing template. SEM images reveal that the CdS microparticle possesses unique surface morphology of wrinkle-like nanotextures which are maintained even after removal of the template. It is suggested that the CdS microparticle consists of the small cubic CdS nanocrystal building blocks which are patterned to the wrinkle-like nanotexture at the outer part including the surface and the bulky agglomerate in the core. In particular, this unique CdS microparticle has the high surface area and the nanoporous nature as well as the characteristic optical responses in visible spectral region. Such unique characteristics of this new CdS polycrystalline microparticle hopefully provide the potential application of a noble photocatalyst which can easily be recycled in heterogeneous photocatalytic reactions.

Acknowledgements

This work was financially supported by a Grant from National Research Laboratory (NRL) (grant No. M1-0302-00-0027) program and a grant from National R&D Project for Nano-Science and Technology (Grant No. M1-0214-00-0021) administered by the Ministry of Science and Technology (MOST). We are grateful for instrumental supports from the equipment facility of CRM-KOSEF, Korea University.

References

[1] A.P. Alivisatos, Science 271 (1996) 933.
[2] Z. Zhong, D. Wang, Y. Cui, M.W. Bockrath, C.M. Lieber, Science 302 (2003) 1377.
[3] S. Sun, C.B. Murray, D. Weller, L. Folks, A. Moser, Science 287 (2000) 1989.
[4] W.U. Huynh, J.J. Dittmer, A.P. Alivisatos, Science 295 (2002) 2425.
[5] K. Lee, Y.-H. Kim, S.B. Han, H. Kang, S. Park, W.S. Seo, J.T. Park, B. Kim, S. Chang, J. Am. Chem. Soc. 125 (2003) 6844.
[6] X. Jiang, Y. Xie, J. Lu, L. Zhu, W. He, Y. Qian, Chem. Mater. 13 (2001) 1213.
[7] P. Zhang, L. Gao, J. Mater. Chem. 13 (2003) 2007.
[8] P.V. Braun, S.I. Stupp, Mater. Res. Bull. 34 (1999) 463.
[9] R.J. Roe, Methods of X-ray and Neutron Scattering in Polymer Science, Oxford University Press, New York, 2000.
[10] N.M. Huang, C.S. Kan, S. Radiman, Appl. Phys. A 76 (2003) 555.
[11] H.P. Klug, L.E. Alexander, X-Ray Diffraction Properties for Polycrystalline and Amorphous Materials, Wiley, New York, 1974.
[12] D.L. Leslie-Pelecky, X.Q. Zhang, S.H. Kim, M. Bonder, R.D. Rieke, Chem. Mater. 10 (1998) 164.
[13] J. Nanda, S. Sapra, D.D. Sarma, N. Chandrasekharan, G. Hodes, Chem. Mater. 12 (2000) 1018.
[14] Y. Nosaka, J. Phys. Chem. 95 (1991) 5054.
[15] R. Rossetti, R. Hull, J.M. Gibson, L.E. Brus, J. Chem. Phys. 82 (1985) 552.
[16] H. Weller, Angew. Chem. Int. Ed. 32 (1993) 41.
[17] Y. Wang, N. Herron, J. Phys. Chem. 95 (1991) 525.
[18] M. O'Neil, J. Marohn, G. McLendon, J. Phys. Chem. 94 (1990) 4356.
[19] W.-S. Chae, J.-H. Ko, I.-W. Hwang, Y.-R. Kim, Chem. Phys. Lett. 365 (2002) 49.
[20] R.C. Weast (Ed.), CRC Handbook of Chemistry and Physics, 70th ed., CRC Press, Boca Raton, FL, 1989, p. B-79.
[21] E.S. Kikkinides, M.E. Kainourgiakis, A.K. Stubos, Langmuir 19 (2003) 3338.
[22] O.Y. Kwon, H.S. Shin, S.W. Choi, Chem. Mater. 12 (2000) 1273.
[23] T. Sasaki, S. Nakano, S. Yamauchi, M. Watanabe, Chem. Mater. 9 (1997) 602.